

ORIGINAL RESEARCH ARTICLE

Fused granular fabrication of conformally cooled injection molding tools

Supplementary File

S1. Mold parts and cooling channels

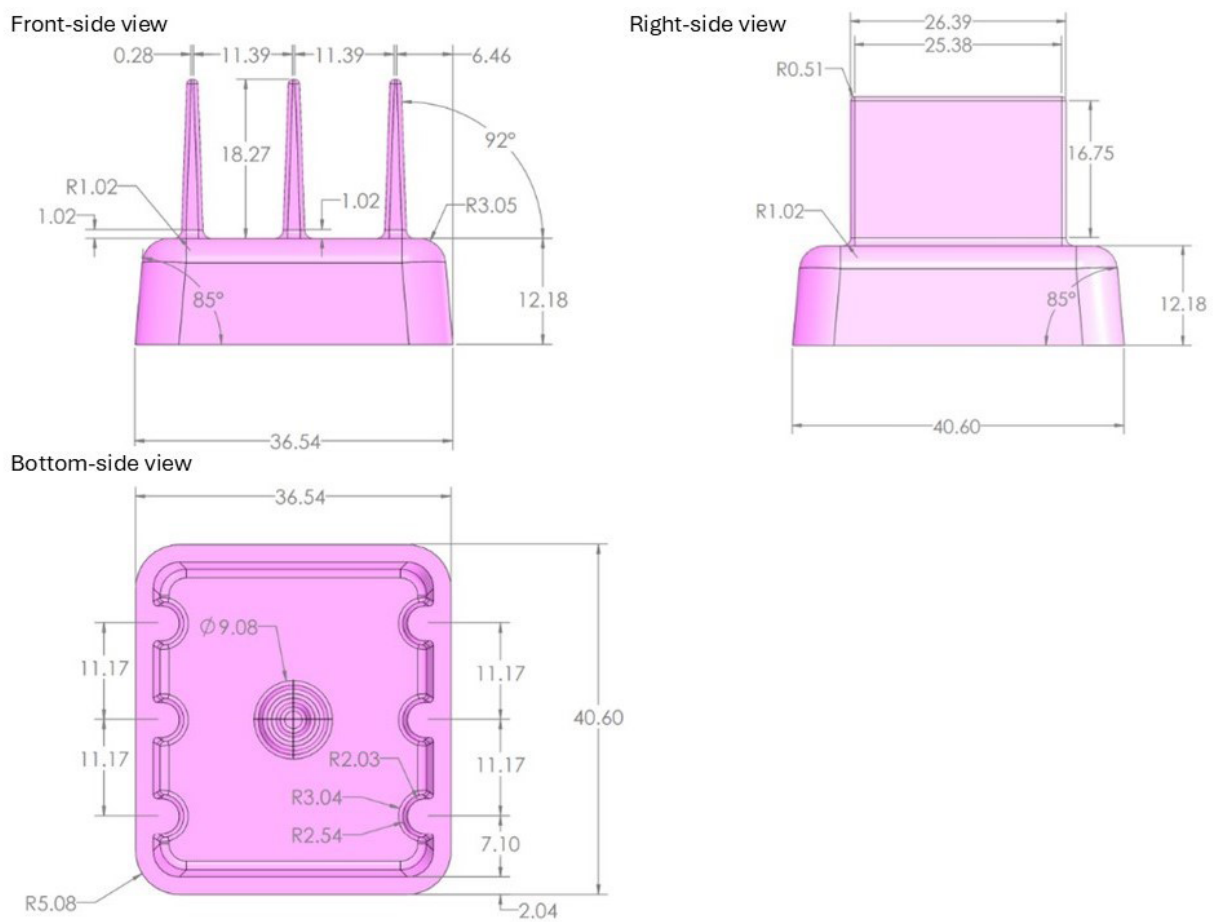


Figure S1. Orthographic projections of the molded part. All dimensions are given in mm

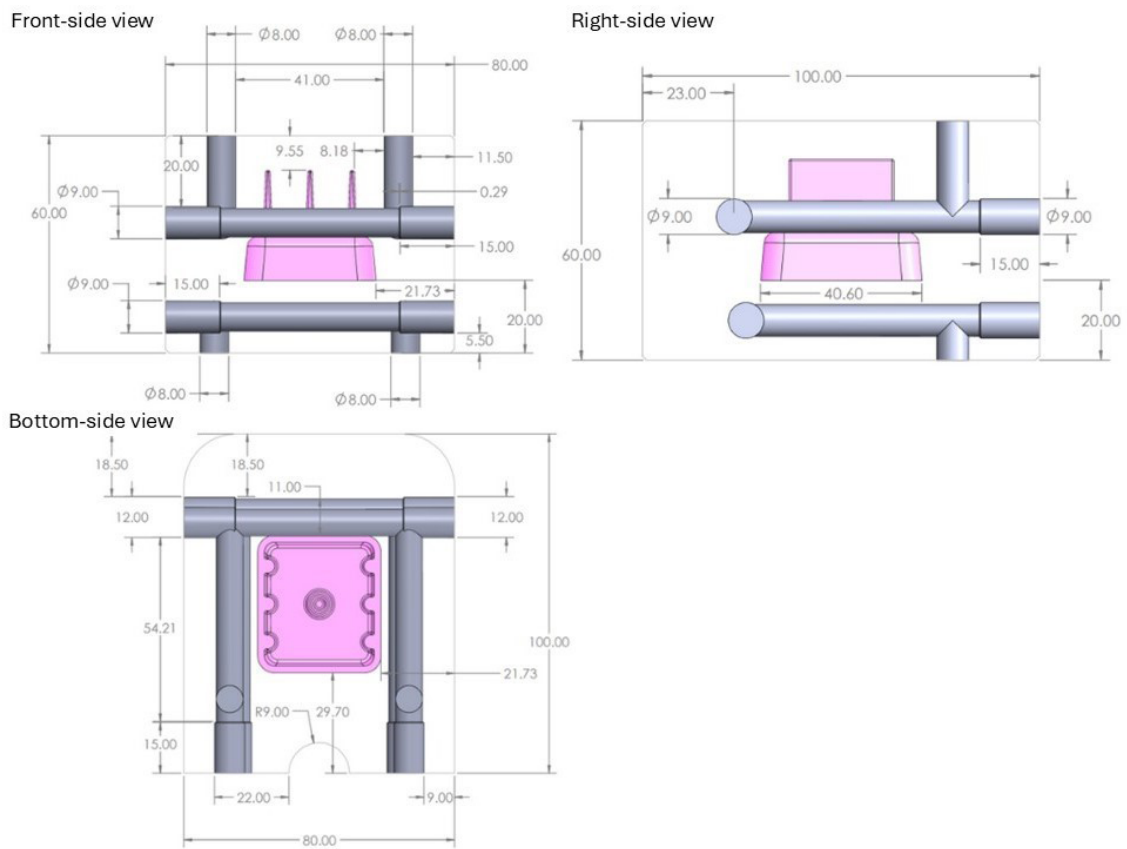


Figure S2. Orthographic projections of the conventional cooling channels. All dimensions are given in mm

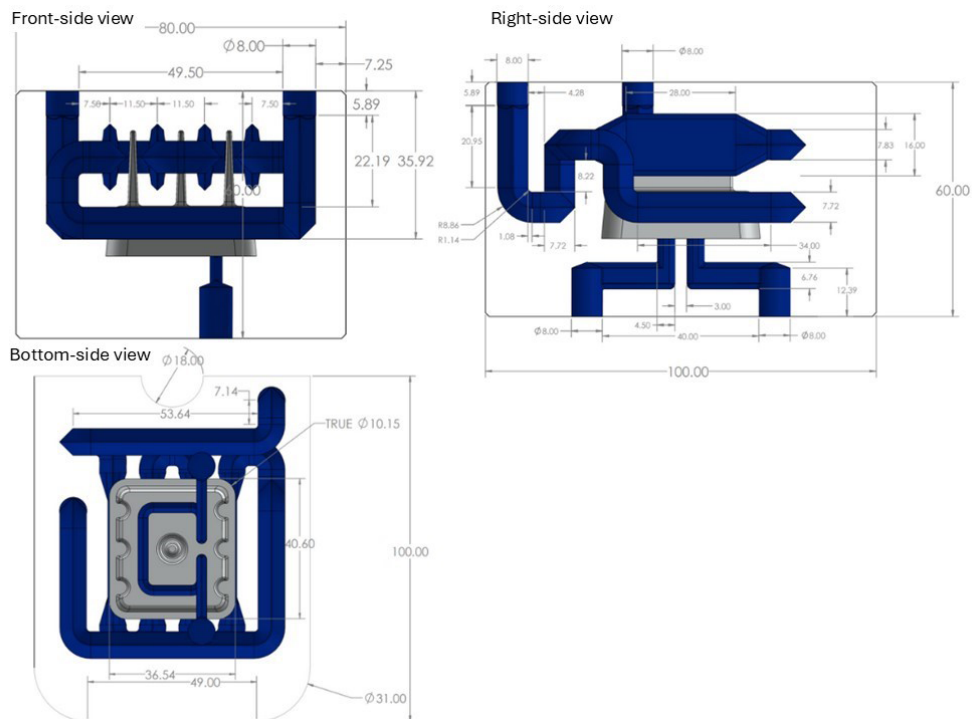


Figure S3. Orthographic projections of the conformal cooling channels. All dimensions are given in mm

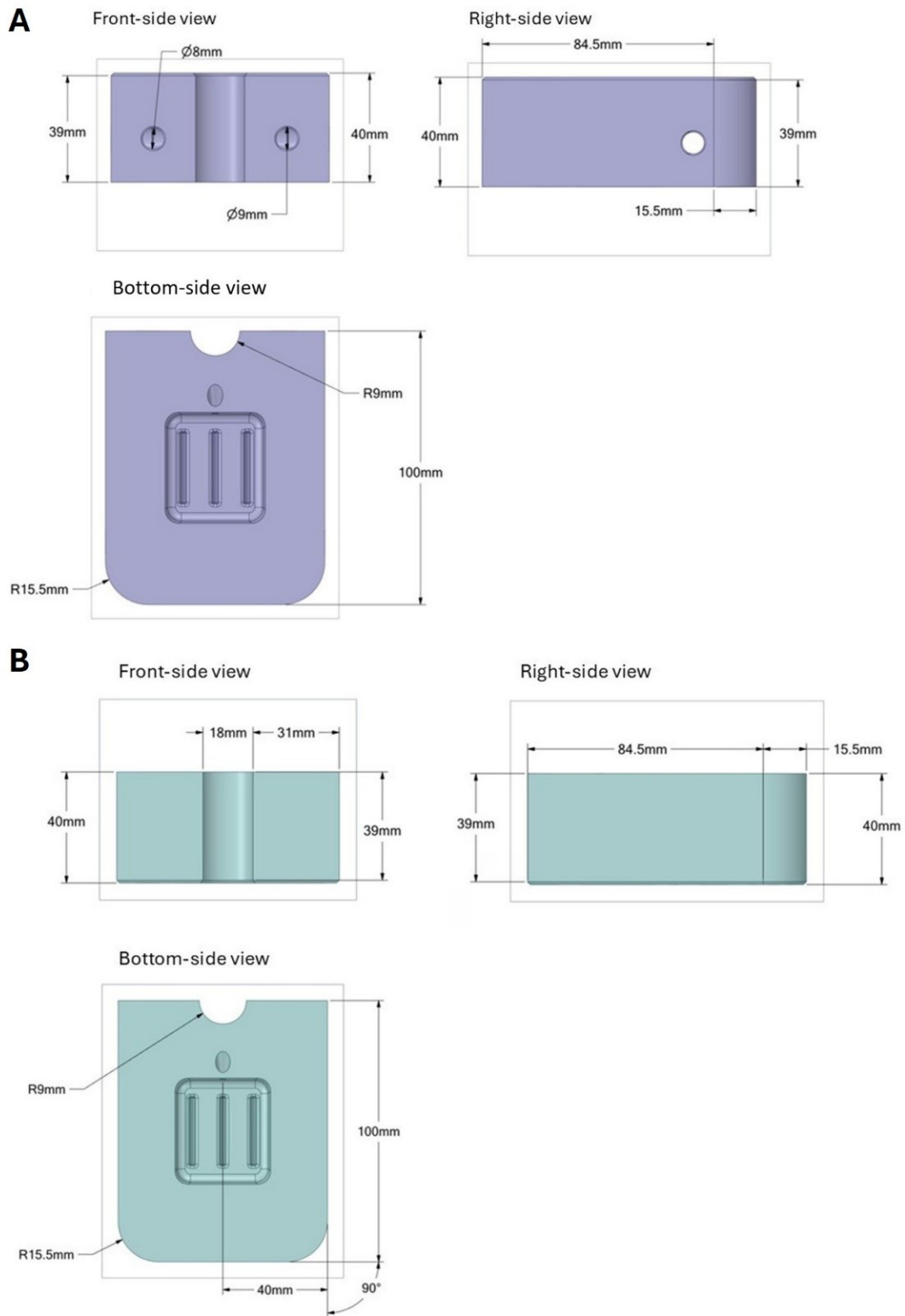


Figure S4. Orthographic projections of the cavity side injection molding component with (A) conventional (B) conformal cooling channel designs

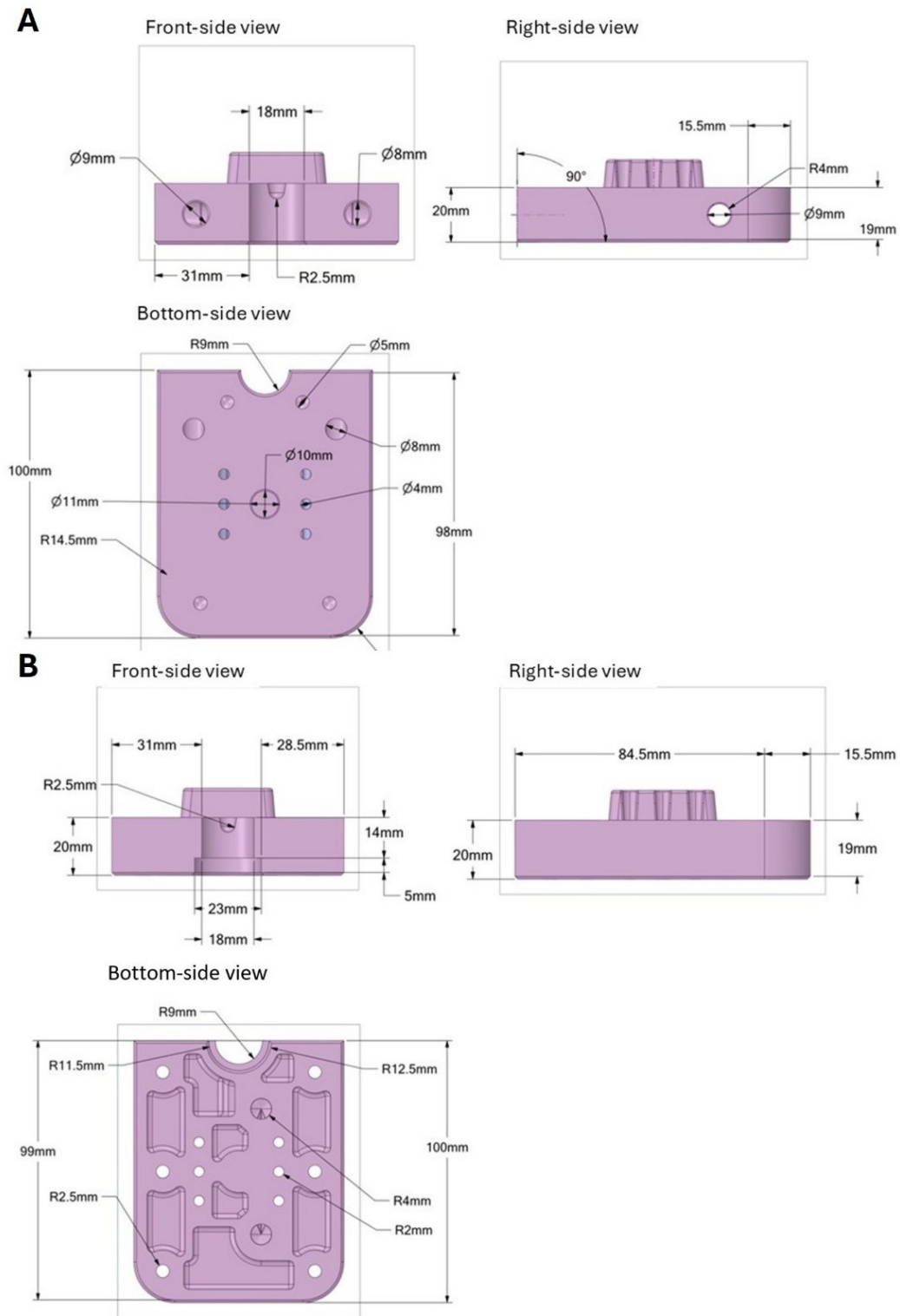


Figure S5. Orthographic projections of the core side injection molding component with (A) conventional (B) conformal cooling channel designs

## S2. Numerical simulation model

### S2.1. Mesh generation and size

The computational domain was discretized in ANSYS Fluent 2020R2 (ANSYS Inc., USA) using a polyhedral mesh. This approach provides faster and more accurate convergence than tetrahedral meshes, as it reduces the overall number of elements while maintaining a high resolution near complicated geometries. The mesh was refined along the tool walls, cooling channels, and polymer–tool interfaces to better capture boundary layer effects and heat transfer gradients.

To investigate the influence of mesh size on solution accuracy and computing efficiency, a mesh sensitivity analysis was performed using element sizes of 5 mm, 4 mm, 3.3 mm, 1 mm, and 0.5 mm (Figure S6). The 1 mm element size offered the optimum balance between spatial resolution and numerical accuracy, capturing steep temperature gradients and transient flow characteristics near tool walls and cooling channels. A coarser mesh resulted in less accurate temperature predictions and smoother thermal distributions, potentially affecting the

accuracy of time-dependent heat transfer computations. As a result, the 1-mm mesh was chosen to provide a more reliable transient solution at an acceptable computational cost. At a grid size of 1 mm, the ANSYS Fluent meshing generated 5.718 million cells and 1.216 million cells for the conformal and conventional designs, respectively.

### S2.2. Solution setup

A coupled pressure-based solver with a time step size of 0.01 s was used for the conventional design and 0.1 s for the conformal design. The coupled scheme simultaneously solves the pressure and velocity equations, ensuring that the velocity field is consistent with the pressure distribution.

Figure S7 displays the effect of different time step sizes on the total average surface temperature for the conformal case. The spatial discretization was performed using a least-squares cell-based gradient method, second-order pressure discretization, and second-order upwind schemes, while a second-order implicit formulation was applied for temporal discretization. The convergence tolerance of the continuity equation was set to  $1 \times 10^{-5}$  to ensure a converged solution. The energy equation was enabled to compute the heat transfer across the numerical domain.

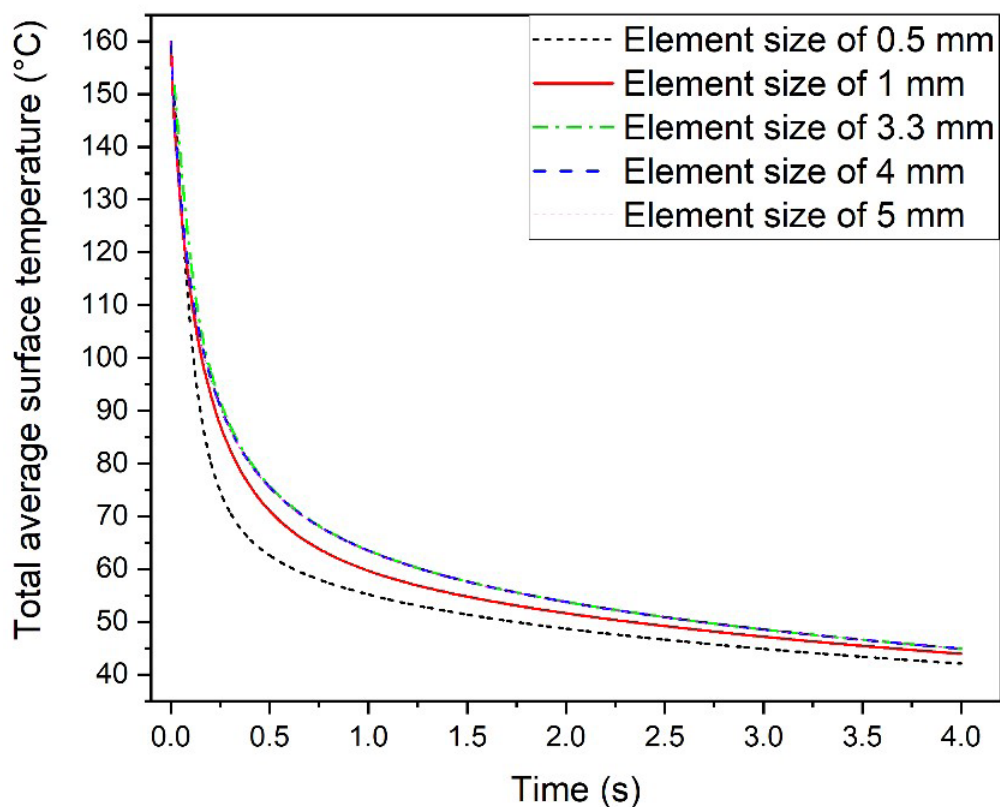


Figure S6. Sensitivity study of element size

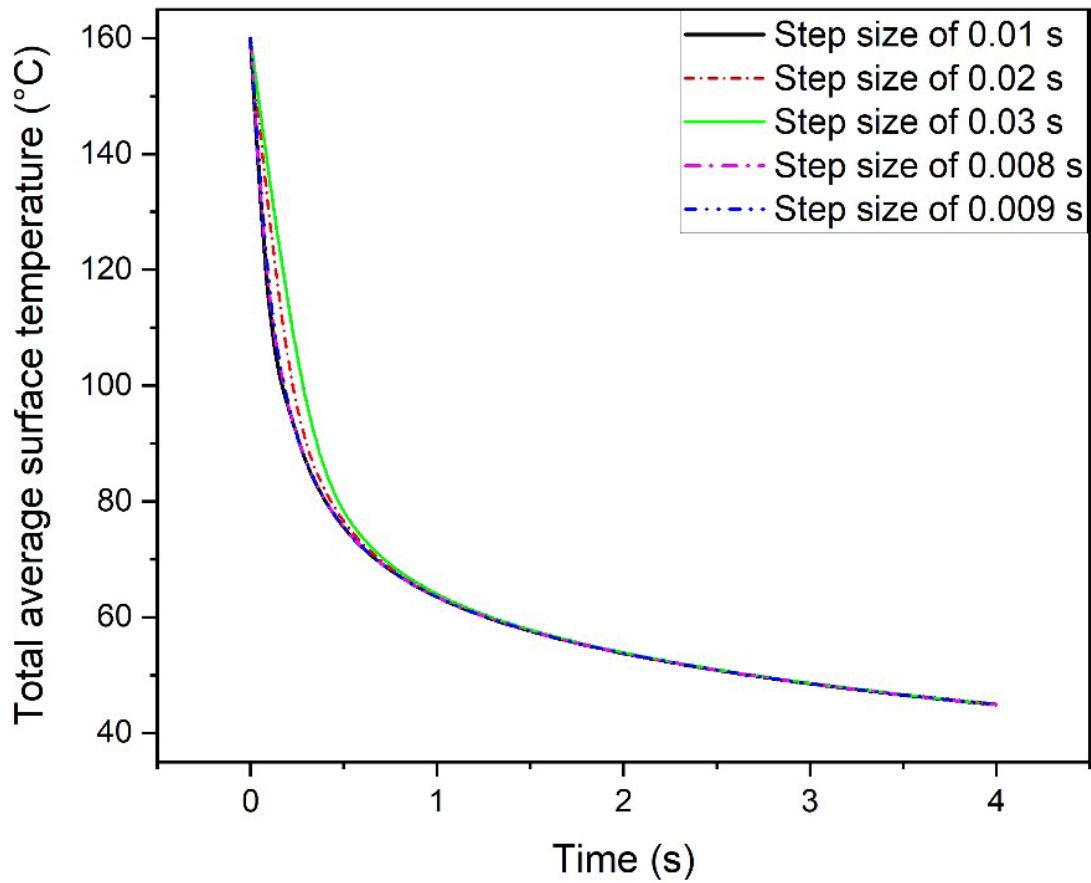


Figure S7. Sensitivity study of time step size (s)

S3. Overhang test

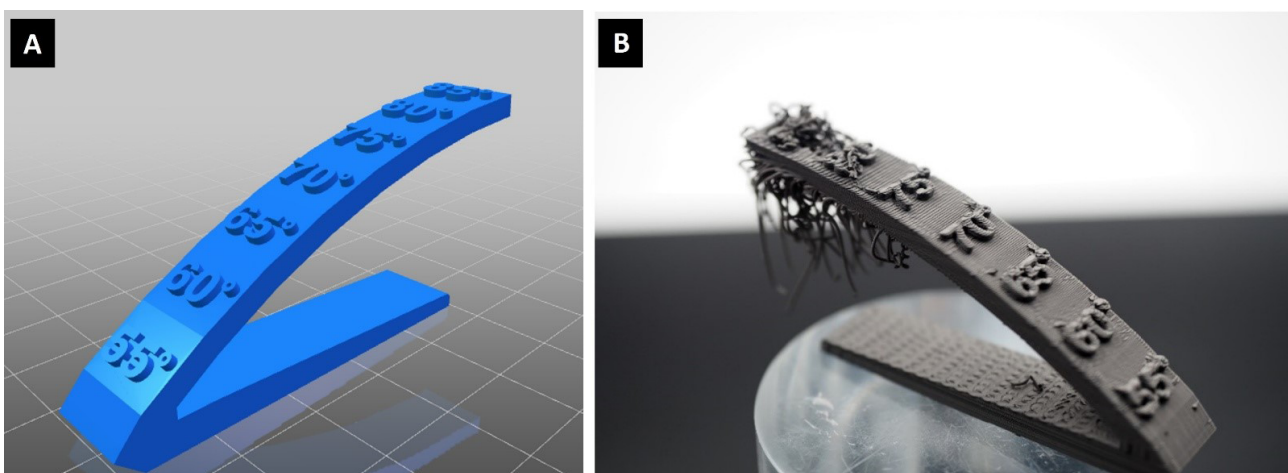


Figure S8. Overhang test geometry: (A) Computer-aided design and (B) the printed part

**S4. Temperature probe at specific points on the mold surface**

Figure S9 examines the temperature variation over a full cycle, based on data from 13 probe locations on a sectional plane for both the conventional and conformal cooling

models.

Figure S9A and S9B presents the sectional views of the conventional and conformal designs, while Figure S9C and S9D illustrates the temperature contours at the end of the cooling cycle ( $t = 20$  s), along with the locations of

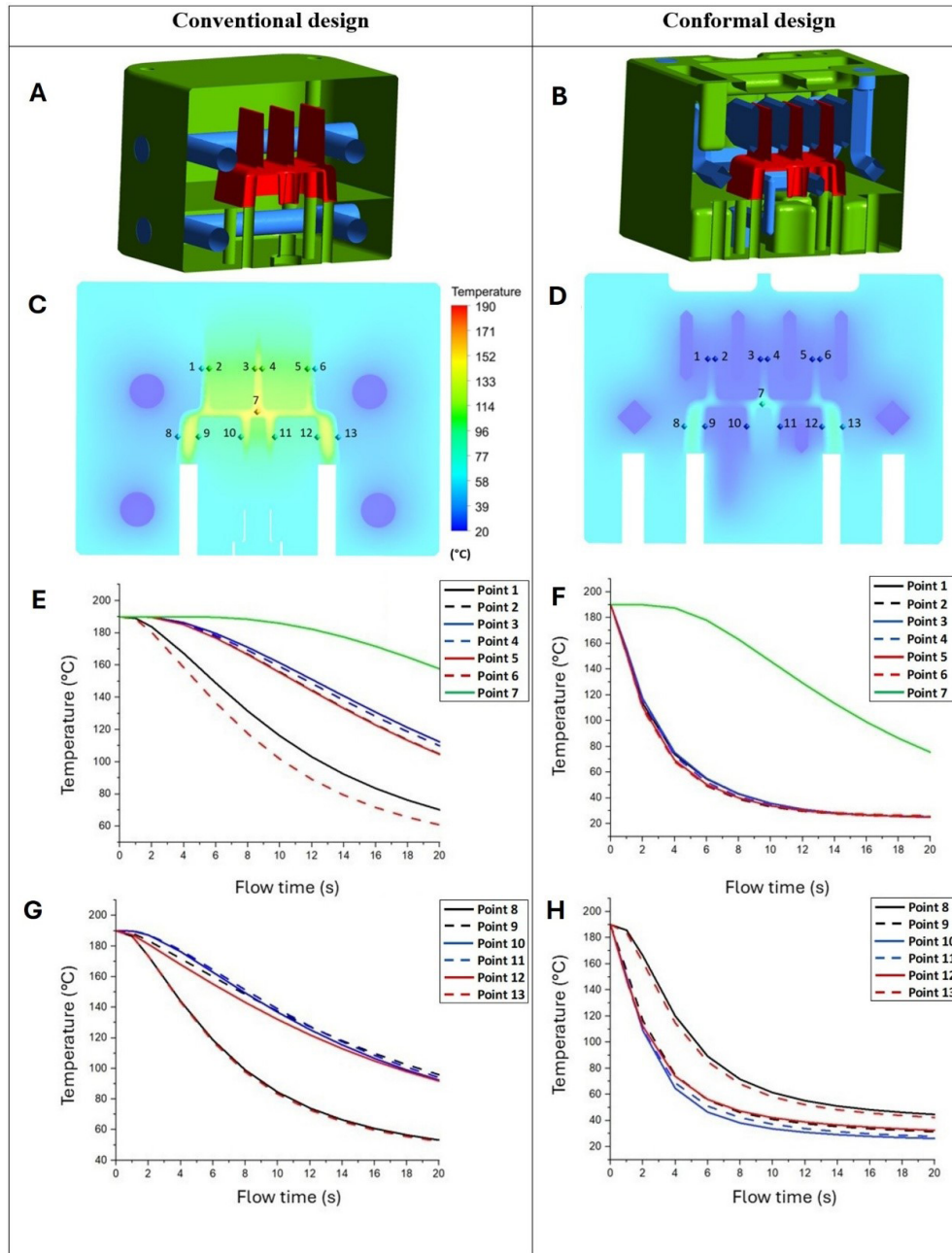


**Figure S9.** Analyzing the cooling process at different probe points on the tool surface. (A,B) Sectional views of the (A) conventional and (B) conformal cooling channel designs, with green indicating the tool body, red representing the molded part, and blue indicating the cooling channels. (C,D) Temperature contours at the section planes at  $t = 20$  s for the (C) conventional and (D) conformal designs, with the locations of specific points on the tool surface indicated. (E,F) Temperature variation during one cooling cycle at selected mid-top and center points of the (E) conventionally and (F) conformally cooled tool. (G,H) Temperature variation during one cooling cycle at selected mid-bottom points of the (G) conventionally and (H) conformally cooled tool.

12 probe points distributed across the tool surface and one additional point (Point 7) positioned at the center of the molded part. By analyzing point pairs located on opposite sides of the tool walls (e.g., points 1–2, 3–4), it is evident that the conformal design provides more uniform cooling. This effect is particularly noticeable on the fins, where temperature differences between opposite wall sides are minimized in the conformal design compared to the conventional design, as illustrated in [Figure S9E–H](#).

Achieving temperature uniformity is essential in cooling channel design, as it helps minimize thermal stresses within the molded part. However, a comparison of the temperature evolution at point pairs 8–9 and

12–13 on the mid-bottom region of the conformal design ([Figure S9H](#)) reveals noticeable differences in their cooling curves, indicating that there is still potential for further optimization of the conformal cooling channel design. In both models, the central point within the molded part (Point 7) exhibits the slowest cooling rate. However, as shown in [Figure S9E–H](#), the final temperature of this point after one cooling cycle is nearly half that in the conformal design compared to the conventional design.

## Supplementary video

**Video S1.** Comparison of the cooling behavior of the two-channel designs over time during one cycle.